Volume 14 | Number 24 | 21 December 2014 | Pages 4577–4698

Lab on a Chip

Miniaturisation for chemistry, physics, biology, materials science and bioengineering

www.rsc.org/loc

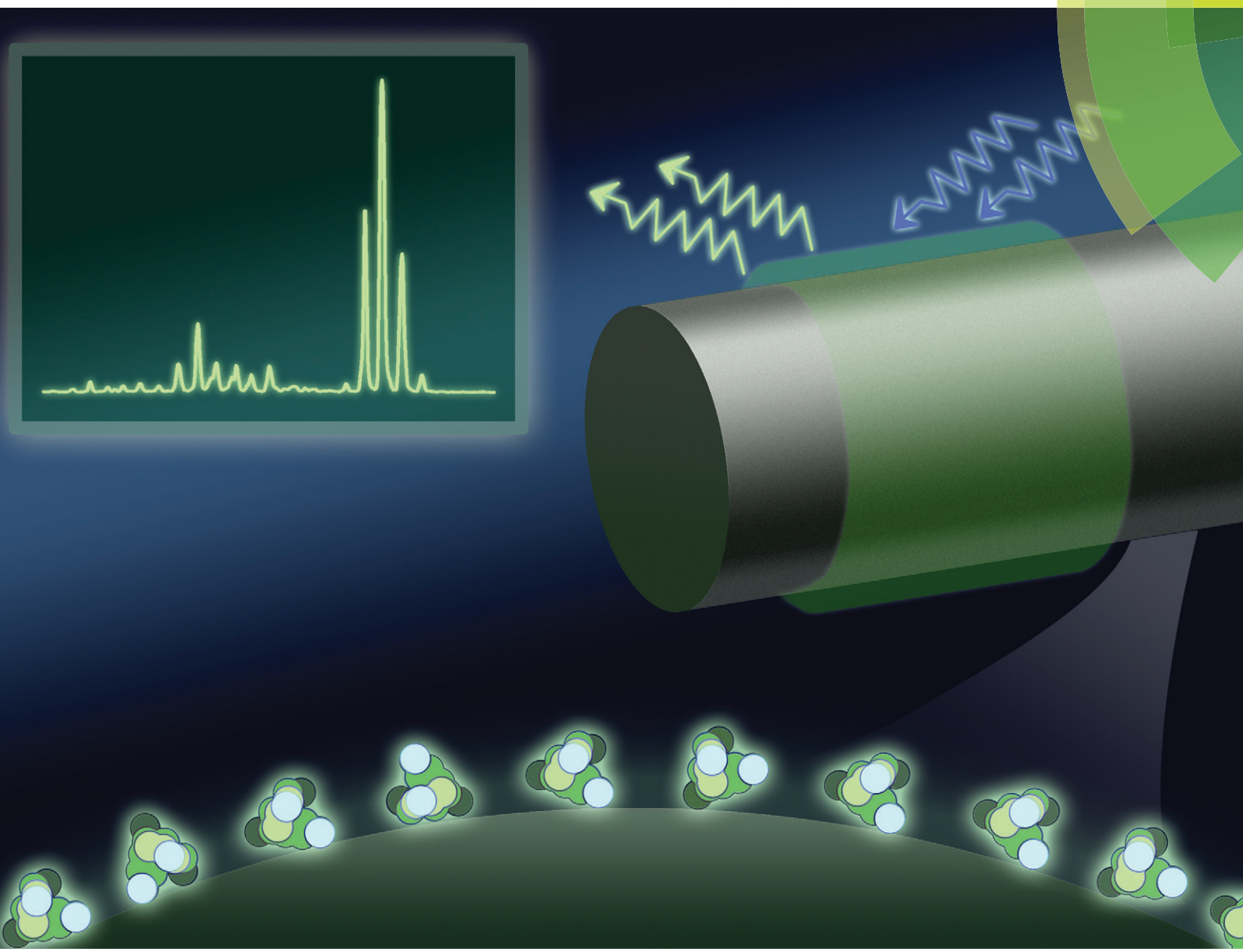

ISSN 1473-0197

ROYAL SOCIETY OF CHEMISTRY

COMMUNICATION
Xudong Fan *et al.*
Optofluidic lasers with a single molecular layer of gain

Lab on a Chip

COMMUNICATION

View Article Online
View Journal | View Issue

Cite this: *Lab Chip*, 2014, **14**, 4590

Received 25th July 2014,
Accepted 2nd October 2014

DOI: 10.1039/c4lc00872c

www.rsc.org/loc

Optofluidic lasers with a single molecular layer of gain†

Qiushu Chen,[a] Michael Ritt,[b] Sivaraj Sivaramakrishnan,[ab] Yuze Sun[c] and Xudong Fan*[a]

We achieve optofluidic lasers with a single molecular layer of gain, in which green fluorescent protein, dye-labeled bovine serum albumin, and dye-labeled DNA, are used as the gain medium and attached to the surface of a ring resonator *via* surface immobilization biochemical methods. It is estimated that the surface density of the gain molecules is on the order of 10^{12} cm^{-2}, sufficient for lasing under pulsed optical excitation. It is further shown that the optofluidic laser can be tuned by energy transfer mechanisms through biomolecular interactions. This work not only opens a door to novel photonic devices that can be controlled at the level of a single molecular layer but also provides a promising sensing platform to analyze biochemical processes at the solid–liquid interface.

Introduction

The optofluidic laser is an emerging technology that integrates the microcavity, microfluidic channel and gain medium in liquid.[1–5] It has a broad range of applications in novel photonic devices, such as on-chip tunable coherent light sources[6–10] and bio-controlled lasers,[11–16] and in sensitively analyzing biomolecules.[2,3,5,17–22] The optofluidic laser exhibits great versatility. Various microcavities have been developed, including Fabry–Pérot cavities,[6,15,18,22] ring resonators,[11,13,14,16,19,21] distributed feedback cavities[8,23] and photonic crystals.[10] Many types of materials, such as organic dyes,[6,8,10,11,13,19,20] biomaterials (fluorescent proteins,[16,18,21] vitamins,[15] luciferins[14]) and products of enzyme–substrate reaction,[22] can be used as the gain medium. To date, nearly all optofluidic lasers are demonstrated with the gain medium dispersed in bulk solution. Consequently, the entire lasing mode present in liquid interacts with the gain medium. For example, for the optofluidic laser based on Fabry–Pérot cavities,[6,15,18] droplets[15,16] and distributed feedback cavities,[8] most of the lasing mode (>90%) is in the gain medium. For those based on ring resonators and photonic crystals, the entire evanescent field (characteristic decay length of approximately 100 nm) resides in the gain medium. Accordingly, bio-control of and bio-analysis with the optofluidic laser need to be accomplished in bulk solution.

Here, we achieve optofluidic lasers with a single molecular layer of gain medium placed at the interface of a solid substrate and liquid. The motivation behind this work is threefold.

First, lack of precise control of the gain medium position may significantly deteriorate the lasing performance. For instance, in the ring resonator case, only 0.1–1% of gain molecules in bulk solution participate in the lasing action. The rest simply contributes to the fluorescence background that affects the quality of laser emission or sensitivity of the bio-analysis.[12,19,20,22] Placing the gain medium at the optimal position for maximal light–matter interaction will not only improve the lasing efficiency and threshold, but also reduce fluorescence background and enable better control of the laser.

Second, the optofluidic laser has been used for bio-analysis,[3,5,12,19–22] which complements the conventional fluorescence-based technologies. There are two generic schemes in fluorescence-based detection – bulk solution detection and surface detection. In the bulk solution detection case, biomolecules move freely in the sample solution. Typical examples include detection with molecular beacons[24] and intercalating dyes.[25] In the surface detection case, biomolecules are immobilized or captured on a solid/liquid interface such as using microbeads.[26] While the optofluidic laser has been quite successful in bulk solution-based detection,[2,3,5,18–22] its surface-based detection capability has

[a] *Department of Biomedical Engineering, University of Michigan, Ann Arbor, MI 48109, USA. E-mail: xsfan@umich.edu*
[b] *Department of Cell and Developmental Biology, University of Michigan, Ann Arbor, MI 48109, USA*
[c] *Department of Electrical Engineering, University of Texas at Arlington, Arlington, TX 76019, USA*

† Electronic supplementary information (ESI) available. See DOI: 10.1039/c4lc00872c

not been explored. Demonstration of an optofluidic laser with a single molecular layer on the solid/liquid interface would be a critical step towards a plethora of studies analogous to those using fluorescence.

Third, the laser with a single molecular layer of gain, which is similar to a semiconductor laser such as VCSEL (vertical-cavity surface-emitting laser) that consists of a single quantum-well layer as the gain medium,[27,28] is fundamentally interesting, as it provides a means to ultimately test the capability and limit of a laser. Indeed, lasing from a thin fluorophore-doped film coated on the resonator surface using various coating methods (*e.g.*, spin-, dip-, or drop-coating) has recently been demonstrated.[29–33] However, those methods result in a coating thickness of approximately 100 nm, equivalent to hundreds of molecular layers. Lasing from a single molecular layer of gain has never been realized.

In this work, using surface immobilization biochemistry we are able to attach a single layer (or even a sub-layer) of gain molecules on the surface of an optical fiber, whose circular cross section serves as the ring resonator (Fig. 1(A)). The whispering gallery modes (WGMs) supported by the ring resonator interact with the gain molecules and provide the optical feedback for lasing. We demonstrate strong lasing emission from enhanced green fluorescent protein (eGFP) and dye-labeled bovine serum albumin (BSA) with a surface density of approximately 10^{12} cm^{-2}. Control of the lasing emission is also achieved using energy transfer *via* DNA hybridization on the surface.

Experimental

An optical fiber (SMF-28, 125 μm in diameter) is chosen to serve as the ring resonator in this work due to its easy preparation, predictable WGM evanescent field distribution near the surface and consistent quality along the axis.[34] The *Q*-factor of this type of ring resonator exceeds 10^6.[35,36] To functionalize the ring resonator surface, the fiber is first sonicated in acetone, ethanol and deionized (DI) water in series, each for 15 minutes. Then the cleaned fiber is immersed in HCl/ethanol (v : v = 1 : 1) for 30 minutes. After rinsing in DI water and drying under air flow, the fiber is silanized with (3-aminopropyl)-trimethoxysilane (3-APTMS, 5% in methanol) for 30 minutes and rinsed with ethanol. Finally, the fiber is cured at 110 °C overnight and stored in a refrigerator at 4 °C for future use. For subsequent attachment of a single layer of gain molecules on the fiber surface, the silanized fiber is activated with the freshly prepared homofunctional amine-to-amine cross-linker bis(sulfosuccinimidyl) suberate (BS^3) (0.1 mg mL^{-1} in phosphate-buffered saline (PBS)) for 30 minutes and rinsed with PBS before incubation with the molecules of interest.

The optofluidic laser setup is illustrated in Fig. 1(B). The fluidic chamber is made of PDMS (polydimethylsiloxane). It has an inlet/outlet for liquid delivery. The fiber is suspended inside the chamber with no contact with the chamber wall. A confocal setup is used to excite the ring resonator with a pulsed optical parametric oscillator (OPO) (repetition rate: 20 Hz, pulse width: 5 ns) and collect the laser emission signals *via* a multi-mode fiber.

Results and discussion

We first test the lasing capability of a single layer of eGFP on the surface. The eGFP sample is purchased from BioVision. Each eGFP has a molecular weight of 32.7 kDa and is shaped like a barrel with a length of 4.2 nm and a diameter of 2.4 nm and a single emission center. The BS^3 activated fiber is inserted into the chamber, which is later filled with 1 μM eGFP in PBS. After 30 minutes of incubation, which covalently binds eGFP molecules to the resonator surface (inset of Fig. 2(A)), 1 mL of PBS solution is flowed through the chamber to wash away the unbound molecules. As a result, only those eGFPs that are cross-linked by BS^3 remain on the surface and form a single or an even sub-layer (considering only partial surface coverage) of gain molecules.

Fig. 2(A) shows the eGFP lasing spectrum with multiple lasing peaks due to the multi-mode nature of the WGMs. As nearly all gain molecules participate in the lasing action, the

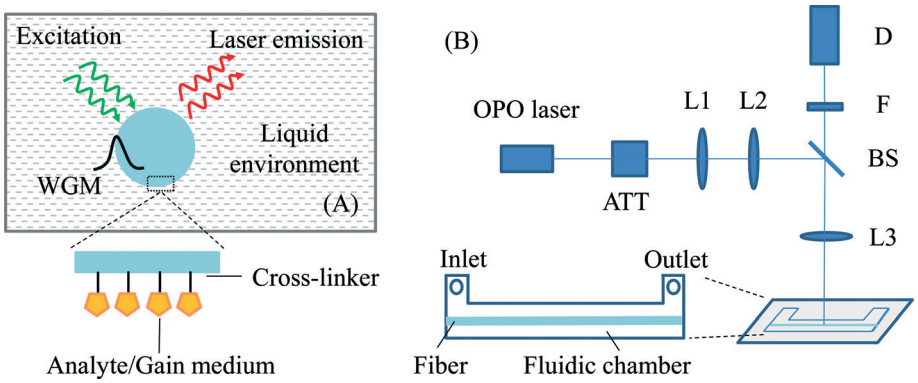

Fig. 1 (A) Cross-sectional view of the ring resonator laser in the liquid environment. WGM: whispering gallery mode. Inset: illustration of a single molecular layer of gain medium attached on the fiber surface through cross-linking chemistry. (B) Schematic of the experimental setup. OPO: optical parametric oscillator; ATT: attenuator; L1/L2/L3: lenses; BS: beam splitter; F: filter; D: detector. Inset: top view of the fluidic chamber. Chamber dimensions: 35 mm × 3 mm × 0.5 mm.

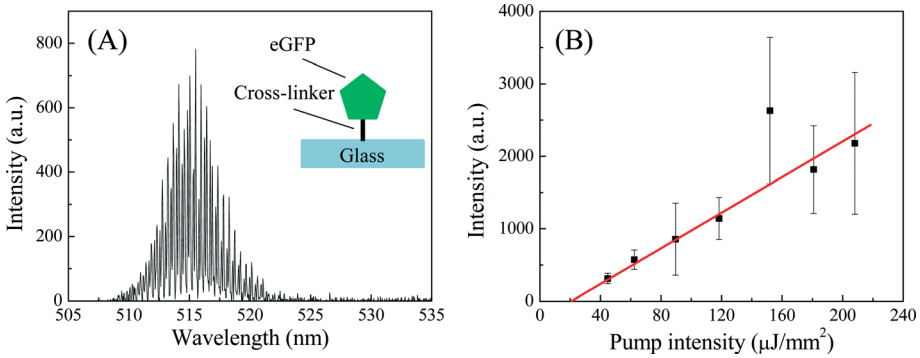

Fig. 2 Lasing characteristics of a single layer of eGFP. (A) Lasing spectrum. Pump intensity is approximately 120 μJ mm^{-2} per pulse. Excitation wavelength: 488 nm. (B) Spectrally integrated eGFP laser output as a function of pump intensity. Spectral integration takes place between 507 nm and 542 nm. Lasing threshold is approximately 23 μJ mm^{-2} per pulse. The solid line is the linear fit above the threshold. Error bars are obtained with 3 measurements.

fluorescence background is negligible. The lasing threshold derived from Fig. 2(B) is approximately 23 μJ mm^{-2}. These results demonstrate that even a single (or sub-) layer of gain molecules is sufficient for lasing. The lasing threshold is on a par with that for the bulk solution-based optofluidic laser using much higher concentrations of eGFP (typically >10 μM).[21] Note that in Fig. 2(B), each measurement in the threshold curve is performed on a different portion of the fiber slightly shifted along its longitudinal axis to eliminate the photo-bleaching effect on the emission intensity. Overall, the gain medium coverage on the fiber is homogenous. Deviation from the linear fit observed for the data points may be attributable to the local inhomogeneity of the gain medium.

Theoretical analysis is carried out to understand the laser process (see details in the ESI†). The lasing threshold can be written as:[19]

$$I_{\text{th}} = \frac{\gamma}{\Gamma - \gamma}, \quad (1)$$

where Γ is the fraction of gain molecules that participate in lasing action ($\kappa = 1$ in the eGFP case). γ is the fraction of gain molecules in the excited state at the threshold,

$$\gamma = \frac{A_1}{A} = \frac{2\pi m_1 L}{\lambda_0 \eta Q_0 \sigma_e(\lambda_0) A}, \quad (2)$$

where A_1 is the surface density of the excited molecules, A is the total surface density, η is the fraction of mode energy in the evanescent field, $\sigma_e(\lambda_0)$ is the eGFP emission cross section at the lasing wavelength, m_1 is the effective refractive index of the circulating optical mode, Q_0 the quality factor of the cavity mode, and L is the penetration depth of the evanescent field. Thus, A/L is the effective bulk solution concentration. The surface density of eGFP for a fully packed surface is about 10^{13} cm^{-2}. Considering the steric hindrance issues, the surface density of eGFP is estimated to be of the order of 10^{12} cm^{-2}, which is similar to the maximal surface coverage of proteins cross-linked on a ring resonator surface obtained in optical label-free measurement.[37] Assuming 100 nm as the evanescent field penetration depth, we can calculate the effective local concentration of eGFP (*i.e.*, A/L) to be approximately 170 μM. Therefore, despite the low concentration (1 μM) used in the experiment, the surface immobilization process results in a much higher local concentration, which is critical for laser operation. Accordingly, γ = 4.3%, similar to that obtained in other dye laser systems (~1–10%).[35,38]

In the above experiment, the eGFPs are attached to the surface non-specifically. We also demonstrate that the lasing can be achieved from a single layer of molecules attached to the surface specifically. To achieve specificity, anti-BSA and dye-labeled BSA (Alexa Fluor®-488) (both from Life Technologies) are used. The BS^3 activated fiber is first incubated with 3 μM anti-BSA PBS solution for 30 minutes. After rinsing with PBS buffer, 1 μM BSA is injected into the chamber and incubated for another 30 minutes. Finally, the fiber is rinsed and filled with PBS buffer before laser tests. Fig. 3(A) is the lasing spectrum of a control fiber on which BSA molecules are cross-linked non-specifically as in the eGFP case. Fig. 3(B) shows the lasing spectrum of specifically bound BSA through anti-BSA. Strong laser emission is observed in both cases. However, specifically bound BSA requires approximately ten times higher pump intensity to achieve the same emission intensity. The difference can be accounted for by the reduced coverage of gain medium on the surface due to multiple immobilization steps, steric hindrance and non-functional anti-BSA on the surface. Based on the theoretical analysis, we can compare Fig. 3(A) and (B) to estimate the BSA/anti-BSA binding. The coverage of BSA through binding with anti-BSA is calculated to be 14% of that through direct non-specific cross-linking (see details in the ESI†).

Going one step further, we show that lasing through a single layer of gain medium can not only be achieved but also be tuned by the fluorescence resonance energy transfer (FRET) mechanism as in the bulk solution case,[12,13] which is critical to biological and biomedical applications, as well as photonic devices. We use DNA for this demonstration due to its simple and robust hybridization mechanism. Two 40 bases long single-stranded DNA sequences are purchased from Integrated DNA Technologies. One is designated as the probe DNA, which is biotinylated at the 5′ end and labeled with Cy3 (donor) at the

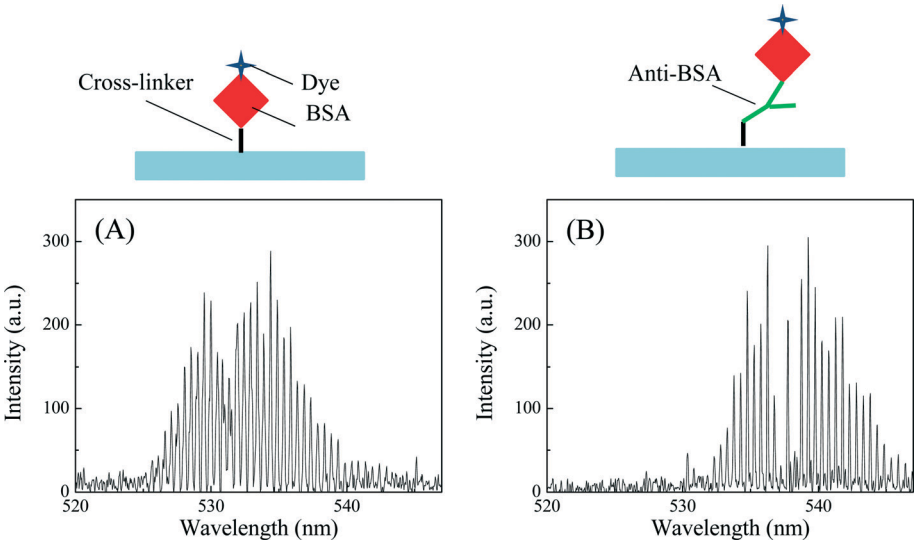

Fig. 3 Lasing spectra from Alexa Fluor®-488-labeled BSA. (A) BSA is immobilized on the ring resonator surface using a cross-linker. Pump intensity: 100 μJ mm^{-2} per pulse. Excitation wavelength: 488 nm. (B) BSA is immobilized on the ring resonator surface *via* binding with anti-BSA. Pump intensity: 1000 μJ mm^{-2} per pulse. Excitation wavelength: 488 nm. Cartoons above the figures illustrate the corresponding immobilization schemes.

3′ end. The other is designated as the target DNA, which is complementary to the probe DNA and labeled with Cy5 (acceptor) at the 5′ end (see Table S1 in the ESI†). The DNA stock solutions are prepared by dissolving the corresponding samples in 500 μL of 1X TAE (tris-acetate-EDTA)/12.5 mM $MgCl_2$, which are further diluted in subsequent experiments. As in the previous experiments, the fiber is activated by BS^3 first. Then 0.5 mg mL^{-1} streptavidin in PBS is introduced into the chamber and incubated with the fiber for 30 minutes followed by sequential PBS, DI water and TAE/$MgCl_2$ buffer rinsing. Finally, 1 μM probe DNA solution is injected and incubated for 30 minutes before TAE/$MgCl_2$ buffer rinsing. Through the well-known biotin–streptavidin interaction, the probe DNA and hence Cy3 molecules are attached to the ring resonator surface.

Fig. 4(A) shows the typical Cy3 lasing spectrum, as expected. Then, 10 nM target DNA solution is injected into the chamber and incubated for 20 minutes, followed by TAE/$MgCl_2$ buffer rinsing. Due to the hybridization of the probe and target DNAs, a fraction of Cy3 molecules on the surface are brought into close proximity of Cy5, resulting in highly efficient (nearly 100%) energy transfer between Cy3 and Cy5 that quenches Cy3 emission. As shown in Fig. 4(B), the laser emission from Cy3 is significantly reduced compared to that in Fig. 4(A), despite the doubled pump intensity. For further Cy3 lasing suppression, 50 nM Cy5-labeled target DNA is introduced. No Cy3 lasing can be observed even with the pump intensity as high as 1000 μJ mm^{-2}. The presence of the target DNA (and hence Cy5) on the surface can be directly verified by Cy5 lasing in Fig. 4(C) during which time Cy3 lasing is suppressed. Alternatively, the reduction in Cy3 lasing emission can also be achieved by hybridizing the probe and target DNA strands in free solution first before immobilizing them on the surface (see Fig. S2 in the ESI†). A quantitative comparison of Cy3 lasing characteristics before and after hybridization with the 10 nM target DNA is plotted in Fig. 4(D). As shown in Fig. S3(A),† the reduction in the laser emission in the presence of the target DNA ranges from 100% (when the pump intensity is below the lasing threshold) to 65% (when the pump intensity is well above the lasing threshold). In contrast, only 20% reduction is obtained with regular fluorescence-based measurement (Fig. S3(B)†). Significant differences between the lasing with and without the target DNA are also evident in lasing threshold and efficiency (Fig. 4(E) and (F)), attesting to the tuning and possible sensing capability of the laser with a single layer of gain on the surface. A simple calculation shows that based on the 3 times difference in the Cy3 lasing threshold before and after 10 nM target DNA incubation, 64% of the immobilized probe DNA is hybridized with the target DNA.

In summary, we have successfully achieved optofluidic lasers with only a single (or even sub-) molecular layer of gain medium. Clean laser emission is observed with virtually no fluorescence background due to well-controlled molecule positions. In addition, due to the maximal light–matter interaction at the solid/liquid interface and the pre-concentration nature of surface immobilization, only 1 μM biomolecules (and hence the fluorophores) is needed to achieve lasing, 10–1000 fold lower than the typical fluorophore concentration used in bulk solution-based optofluidic lasers.[6,8,35,36] Furthermore, the optofluidic laser can be tuned using FRET through biomolecular binding. Finally, threshold analysis based on the laser theory provides a simple means for us to estimate biomolecular surface coverage.

Since all of the gain molecules are accessible from outside in a laser with a single layer of gain, any external stimuli are

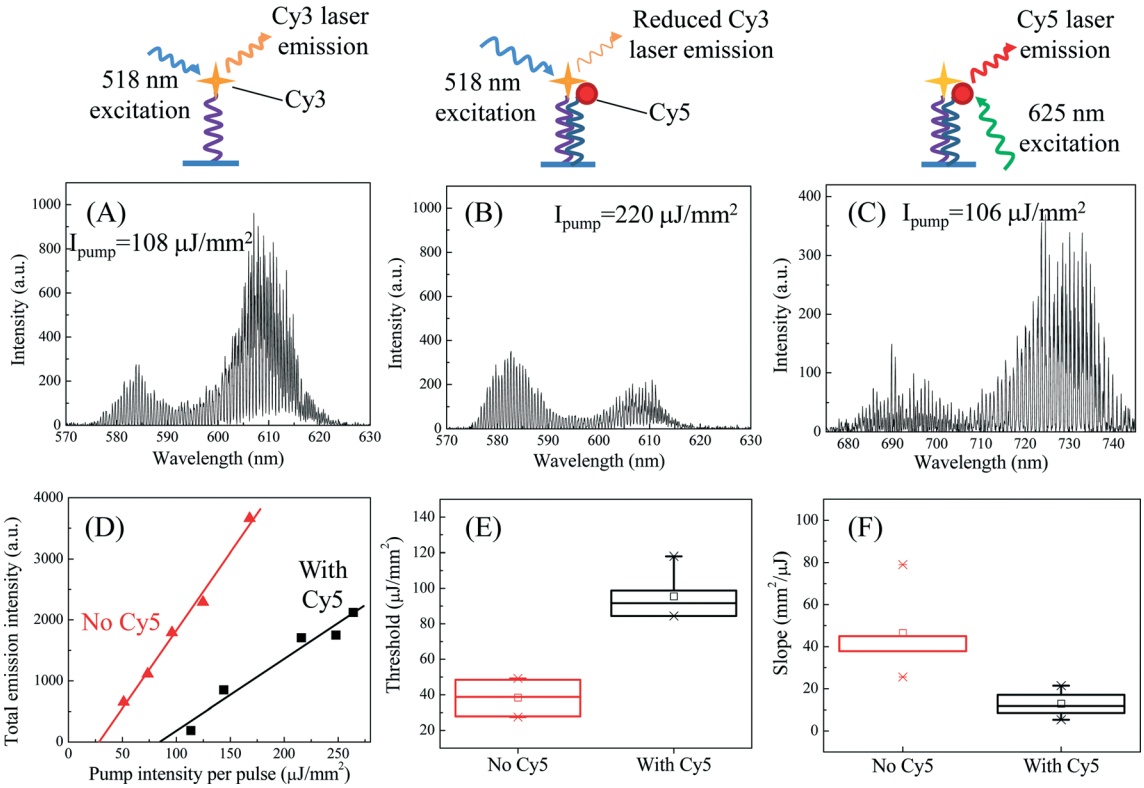

Fig. 4 Comparison of donor (Cy3) laser emission in the absence and presence of acceptor (Cy5). (A) Laser emission from Cy3 in the absence of Cy5. Pump intensity: 108 μJ mm^{-2} per pulse. Excitation wavelength: 518 nm. (B) Laser emission from Cy3 in the presence of Cy5. Pump intensity: 220 μJ mm^{-2} per pulse. Excitation wavelength: 518 nm. (C) Laser emission from Cy5. Pump intensity: 106 μJ mm^{-2} per pulse. Excitation wavelength: 625 nm. Cartoons above (A)–(C) illustrate the corresponding immobilization schemes. (D) Spectrally integrated Cy3 laser output as a function of pump intensity in the absence (triangles) and presence (squares) of Cy5. Spectral integration takes place between 563 nm and 637 nm using the laser emission spectra similar to those shown in (A) and (B). Solid lines are the curve fit above the respective thresholds, showing a threshold of 28 μJ mm^{-2} and 84 μJ mm^{-2}, and a lasing slope of 25 mm^2 μJ^{-1} and 12 mm^2 μJ^{-1}, respectively, for the Cy3 laser in the absence and presence of Cy5. (E) and (F) Lasing threshold and slope obtained with the corresponding curves similar to those plotted in (D), respectively. Error bars are generated with 5 measurements.

expected to cause a rapid and drastic change in the laser gain and hence the laser output characteristics. Therefore, we envision that the work presented here will lead to the development of novel photonic devices that can be sensitively controlled at the level of a single molecular layer. Meanwhile, the potential of bio-sensing can also be explored to complement the traditional fluorescence-based bioanalysis. Currently, the total number of gain molecules participating in the laser action is about 10 million (assuming a surface area of 1000 μm^2). With further reduction in the resonator dimensions using nanophotonic technologies, it may be possible to achieve detection of a small number of molecules, in which changes in only one or a few gain molecules may cause an appreciable change in laser output characteristics.

Acknowledgements

The authors thank financial support from the National Institutes of Health (1R21EB016783) and the discussion from David Burke and Rizal Hariadi.

References

1 Z. Li and D. Psaltis, Optofluidic dye lasers, *Microfluid. Nanofluid.*, 2007, **4**, 145–158.
2 Y. Chen, L. Lei, K. Zhang, J. Shi, L. Wang, H. Li, X. M. Zhang, Y. Wang and H. L. W. Chan, Optofluidic microcavities: Dye-lasers and biosensors, *Biomicrofluidics*, 2010, **4**, 043002.
3 X. Fan and I. M. White, Optofluidic Microsystems for Chemical and Biological Analysis, *Nat. Photonics*, 2011, **5**, 591–597.
4 H. Schmidt and A. R. Hawkins, The photonic integration of non-solid media using optofluidics, *Nat. Photonics*, 2011, **5**, 598–604.
5 X. Fan and S.-H. Yun, The potential of optofluidic biolasers, *Nat. Methods*, 2014, **11**, 141–147.
6 B. Helbo, A. Kristensen and A. Menon, A micro-cavity fluidic dye laser, *J. Micromech. Microeng.*, 2003, **13**, 307–311.
7 Q. Kou, I. Yesilyurt and Y. Chen, Collinear dual-color laser emission from a microfluidic dye laser, *Appl. Phys. Lett.*, 2006, **88**, 091101.

8 Z. Li, Z. Zhang, T. Emery, A. Scherer and D. Psaltis, Single mode optofluidic distributed feedback dye laser, *Opt. Express*, 2006, **14**, 696–701.
9 S. K. Y. Tang, Z. Li, A. R. Abate, J. J. Agresti, D. A. Weitz, D. Psaltis and G. M. Whitesides, A multi-color fast-switching microfluidic droplet dye laser, *Lab Chip*, 2009, **9**, 2767–2771.
10 B. Zhen, S.-L. Chua, J. Lee, A. W. Rodriguez, X. Liang, S. G. Johnson, J. D. Joannopoulos, M. Soljačić and O. Shapira, Enabling enhanced emission and low-threshold lasing of organic molecules using special Fano resonances of macroscopic photonic crystals, *Proc. Natl. Acad. Sci. U. S. A.*, 2013, **110**, 13711–13716.
11 Y. Sun, S. I. Shopova, C.-S. Wu, S. Arnold and X. Fan, Bioinspired optofluidic FRET lasers via DNA scaffolds, *Proc. Natl. Acad. Sci. U. S. A.*, 2010, **107**, 16039–16042.
12 X. Zhang, W. Lee and X. Fan, Bio-switchable optofluidic lasers based on DNA Holliday junctions, *Lab Chip*, 2012, **12**, 3673–3675.
13 Q. Chen, H. Liu, W. Lee, Y. Sun, D. Zhu, H. Pei, C. Fan and X. Fan, Self-assembled DNA tetrahedral optofluidic lasers with precise and tunable gain control, *Lab Chip*, 2013, **13**, 3351–3354.
14 X. Wu, Q. Chen, Y. Sun and X. Fan, Bio-inspired optofluidic lasers with luciferin, *Appl. Phys. Lett.*, 2013, **102**, 203706.
15 S. Nizamoglu, M. C. Gather and S. H. Yun, All-Biomaterial Laser using Vitamin and Biopolymers, *Adv. Mater.*, 2013, **25**, 5943–5947.
16 A. Jonáš, M. Aas, Y. Karadag, S. Manioğlu, S. Anand, D. McGloin, H. Bayraktarc and A. Kiraz, In vitro and in vivo biolasing of fluorescent proteins suspended in liquid microdroplet cavities, *Lab Chip*, 2014, **14**, 3093–3100.
17 J. C. Galas, C. Peroz, Q. Kou and Y. Chen, Microfluidic dye laser intracavity absorption, *Appl. Phys. Lett.*, 2006, **89**, 224101.
18 M. C. Gather and S. H. Yun, Single-cell biological lasers, *Nat. Photonics*, 2011, **5**, 406–410.
19 Y. Sun and X. Fan, Distinguishing DNA by Analog-to-Digital-like Conversion by Using Optofluidic Lasers, *Angew. Chem., Int. Ed.*, 2012, **51**, 1236–1239.
20 W. Lee and X. Fan, Intracavity DNA Melting Analysis with Optofluidic Lasers, *Anal. Chem.*, 2012, **84**, 9558–9563.
21 Q. Chen, X. Zhang, Y. Sun, M. Ritt, S. Sivaramakrishnan and X. Fan, Highly sensitive fluorescent protein FRET detection using optofluidic lasers, *Lab Chip*, 2013, **13**, 2679–2681.
22 X. Wu, M. K. Khaing Oo, K. Reddy, Q. Chen, Y. Sun and X. Fan, Optofluidic laser for dual-mode sensitive biomolecular detection with a large dynamic range, *Nat. Commun.*, 2014, **5**, 3779.
23 W. Song, A. E. Vasdekis, Z. Li and D. Psaltis, Optofluidic evanescent dye laser based on a distributed feedback circular grating, *Appl. Phys. Lett.*, 2009, **94**, 161110.
24 S. Tyagi and F. R. Kramer, Molecular beacons: probes that fluoresce upon hybridization, *Nat. Biotechnol.*, 1996, **14**, 303–308.
25 L. Zhou, L. Wang, R. Palais, R. Pryor and C. Wittwer, High-resolution DNA melting analysis for simultaneous mutation scanning and genotyping in solution, *Clin. Chem.*, 2005, **51**, 1770–1777.
26 S. Brenner, M. Johnson, J. Bridgham, G. Golda, D. H. Lloyd, D. Johnson, S. Luo, S. McCurdy, M. Foy, M. Ewan, R. Roth, D. George, S. Eletr, G. Albrecht, E. Vermaas, S. R. Williams, K. Moon, T. Burcham, M. Pallas, R. B. DuBridge, J. Kirchner, K. Fearon, J.-I. Mao and K. Corcoran, Gene expression analysis by massively parallel signature sequencing (MPSS) on microbead arrays, *Nat. Biotechnol.*, 2000, **18**, 630–634.
27 M. C. Larson, M. Kondow, T. Kitatani, Y. Yazawa and M. Okai, Room temperature continuous-wave photopumped operation of 1.22 μm GaInNAs/GaAs single quantum well vertical-cavity surface-emitting laser, *Electron. Lett.*, 1997, **33**, 959–960.
28 W. Li, T. Jouhti, C. S. Peng, J. Konttinen, P. Laukkanen, E.-M. Pavelescu, M. Dumitrescu and M. Pessa, Low-threshold-current 1.32-μm GaInNAs/GaAs single-quantum-well lasers grown by molecular-beam epitaxy, *Appl. Phys. Lett.*, 2001, **79**, 3386–3388.
29 V. Bulović, V. G. Kozlov, V. B. Khalfin and S. R. Forrest, Transform-Limited, Narrow-Linewidth Lasing Action in Organic Semiconductor Microcavities, *Science*, 1998, **279**, 553–555.
30 A. Rose, Z. Zhu, C. F. Madigan, T. M. Swager and V. Bulovic, Sensivity gains in chemosensing by lasing action in organic polymers, *Nature*, 2005, **434**, 876–879.
31 U. Bog, T. Laue, T. Grossmann, T. Beck, T. Wienhold, B. Richter, M. Hirtz, H. Fuchs, H. Kalt and T. Mappes, On-chip microlasers for biomolecular detection via highly localized deposition of a multifunctional phospholipid ink, *Lab Chip*, 2013, **13**, 2701–2707.
32 C. Dang, J. Lee, C. Breen, J. S. Steckel, S. Coe-Sullivan and A. Nurmikko, Red, green and blue lasing enabled by single-exciton gain in colloidal quantum dot films, *Nat. Nanotechnol.*, 2012, **7**, 335–339.
33 V. D. Ta, R. Chen and H. D. Sun, Tuning Whispering Gallery Mode Lasing from Self-Assembled Polymer Droplets, *Sci. Rep.*, 2013, **3**, 1362.
34 A. Boleininger, T. Lake, S. Hami and C. Vallance, Whispering Gallery Modes in Standard Optical Fibres for Fibre Profiling Measurements and Sensing of Unlabelled Chemical Species, *Sensors*, 2010, **10**, 1765–1781.
35 H.-J. Moon, Y.-T. Chough and K. An, Cylindrical Microcavity Laser Based on the Evanescent-Wave-Coupled Gain, *Phys. Rev. Lett.*, 2000, **85**, 3161–3164.
36 S. I. Shopova, H. Zhu, X. Fan and P. Zhang, Optofluidic ring resonator based dye laser, *Appl. Phys. Lett.*, 2007, **90**, 221101.
37 H. Zhu, I. M. White, J. D. Suter, P. S. Dale and X. Fan, Analysis of biomolecule detection with optofluidic ring resonator sensors, *Opt. Express*, 2007, **15**, 9139–9146.
38 S. Lacey, I. M. White, Y. Sun, S. I. Shopova, J. M. Cupps, P. Zhang and X. Fan, Versatile opto-fluidic ring resonator lasers with ultra-low threshold, *Opt. Express*, 2007, **15**, 17433–17442.